High-Resolution Rooftop Solar PV Potential Assessment Using an Open-Source Remote Sensing Data and Cloud Computing: A Case Study in Padang Utara Subdistrict

Surya Hafizh[a], Widya Prarikeslan[a,*]
[a]Department of Geography, Universitas Negeri Padang, Padang 25132, Indonesia

*Corresponding author: widya_geo@fis.unp.ac.id

Abstract. High-resolution assessment of rooftop solar photovoltaic (PV) potential in urban areas is often constrained by the high cost of commercial data like LiDAR and the computational intensity of analyzing complex geometries. This study develops and applies a novel, fully open-source remote sensing workflow that leverages cloud computing to overcome these limitations. The methodology integrates open-source building and canopy height data to generate a Digital Surface Model (DSM) and introduces a novel Urban Geometric Correction Factor (UGCF). The UGCF combines a multi-temporal Shading Factor, calculated efficiently in Google Earth Engine (GEE), with a Sky View Factor (SVF) to realistically model solar irradiance on individual rooftops. Applied to the complex urban morphology of Padang Utara, Indonesia, the workflow identified significant potential, with 47.17% of viable rooftops classified as 'Optimal' or 'Very Optimal', with a radiation value range of 758.8–848.63 kWh/m²/year. Spatially, the highest potential is concentrated in lower-profile residential areas, not necessarily on the tallest buildings, Critically revealed that internal roof shading is a dominant limiting factor for large buildings. This research presents a cost-effective and replicable methodology, contributing a significant tool for detailed urban solar potential assessment and supporting data-driven sustainable energy planning.

Keywords: Cloud computing; High-Resolution Mapping; Open-source Remote Sensing Rooftop Solar Potential; Urban Geometric Correction.

I. INTRODUCTION

The transition to clean and affordable energy has become an urgent necessity. The energy sector contributes significantly to carbon dioxide emissions, accounting for 34% of global emissions [1]. The high dependence on fossil-based energy sources is the main cause of this condition [1], which makes the energy sector play a vital role in efforts to reduce the effects of climate change due to increasing greenhouse gases [2], [3].

Countries around the world have highlighted the importance of this issue and have formulated common goals in the transition to clean energy as outlined in the Sustainable Development Goals (SDGs), particularly in point 7, which is to achieve clean and affordable energy by 2030 [4].

Indonesia has also adopted this goal, as reflected in Presidential Regulation No. 112 of 2022 concerning the Acceleration of Renewable Energy Development for Electricity Supply and Minister of Energy and Mineral Resources Regulation No. 10 of 2025 concerning the Road Map for the for the Electricity Sector Energy Transition, which is committed to achieving Net Zero Emissions by 2060 [5]. The implementation of this clean energy transition is realized through the use of clean energy as the main source of electricity. One of the most promising sources of clean energy for urban areas today is rooftop solar photovoltaic (PV) [6].

The use of rooftop solar PV in urban areas has become a promising alternative solution in efforts to reduce carbon emissions in the energy sector in urban environments [7]. Roof-mounted solar power systems can reduce the workload of conventional electricity grids and do not require large areas of land as they can utilize available rooftops [8], [9]. This condition is also supported by Indonesia's highly potential location.

Indonesia's location near the equator means that solar radiation is abundant and tends to be stable throughout the year. With an average daily global horizontal irradiance (GHI) of 4.8 Kwh/m^2, the potential for developing rooftop solar PV in this country is very feasible [10]. However, in reality, this condition still faces various significant challenges.

In more detailed studies, LiDAR data is used to model urban geometry and analyze the effects of shadows and sky view factors on the location of rooftop solar power plants. The LiDAR method can produce more detailed and realistic analyses, but it tends to be expensive, requires large computing capacity, and takes a relatively long time, making it relatively difficult to replicate in other areas with limited resources [11], [12], [13], [14], [15]. To address these challenges, innovative solutions are needed, one of which is to utilize open source data and cloud computing technology.

Currently, there is a wealth of detailed open source data and cloud computing platforms available that can be utilized in detailed processing and analysis. One example is the Google Open Building 2.5D and Global Canopy Height data developed by Google, WRI, and Meta [16], [17]. This data has an resolution 1 meters, which can be combined into a Digital Surface Model (DSM) and used freely to support the development of various urban analyses. In data analysis, Google Earth Engine (GEE) is also a promising option for cloud-based spatial data processing. GEE is an open-access cloud computing platform that connects to various open source data without the need to download large datasets, thereby saving local resources and memory [18]. In addition, this platform also provides various ready-to-use functions and algorithms that can assist with various data analysis needs, making it very helpful for more effective and efficient computing. Data and analysis from this platform can be integrated with solar radiation data from the Himawari-8 satellite and meteorological data such as temperature and wind, enabling the calculation of meteorological correction factors and urban geometric correction factors, which form the basis for determining the optimal location for rooftop solar PV [16], [17], [18].

In Indonesia itself, there has not been much detailed research that integrates open-source remote sensing data with cloud computing in determining the potential of rooftop solar PV in urban areas. Therefore, this study offers a new workflow that can integrate these two factors. This integration not only addresses the challenges of cost and availability of commercial data such as LiDAR, but also enables complex urban geometry analysis to be calculated more effectively and efficiently through the Google Earth Engine platform. The contribution of this research is expected to serve as a basis for policymakers in data-driven sustainable energy planning, thereby helping to determine the optimal location for rooftop solar PV in an effort to achieve clean and affordable energy goals in urban areas.

II. METHODOLOGY

2.1 Research Location

The research location is in Padang Utara Subdistrict, Padang City. It is located at 00°53'22“ S – 00°56'8” S and 100°20'31“ E – 100°22'40” E. Padang Utara Subdistrict

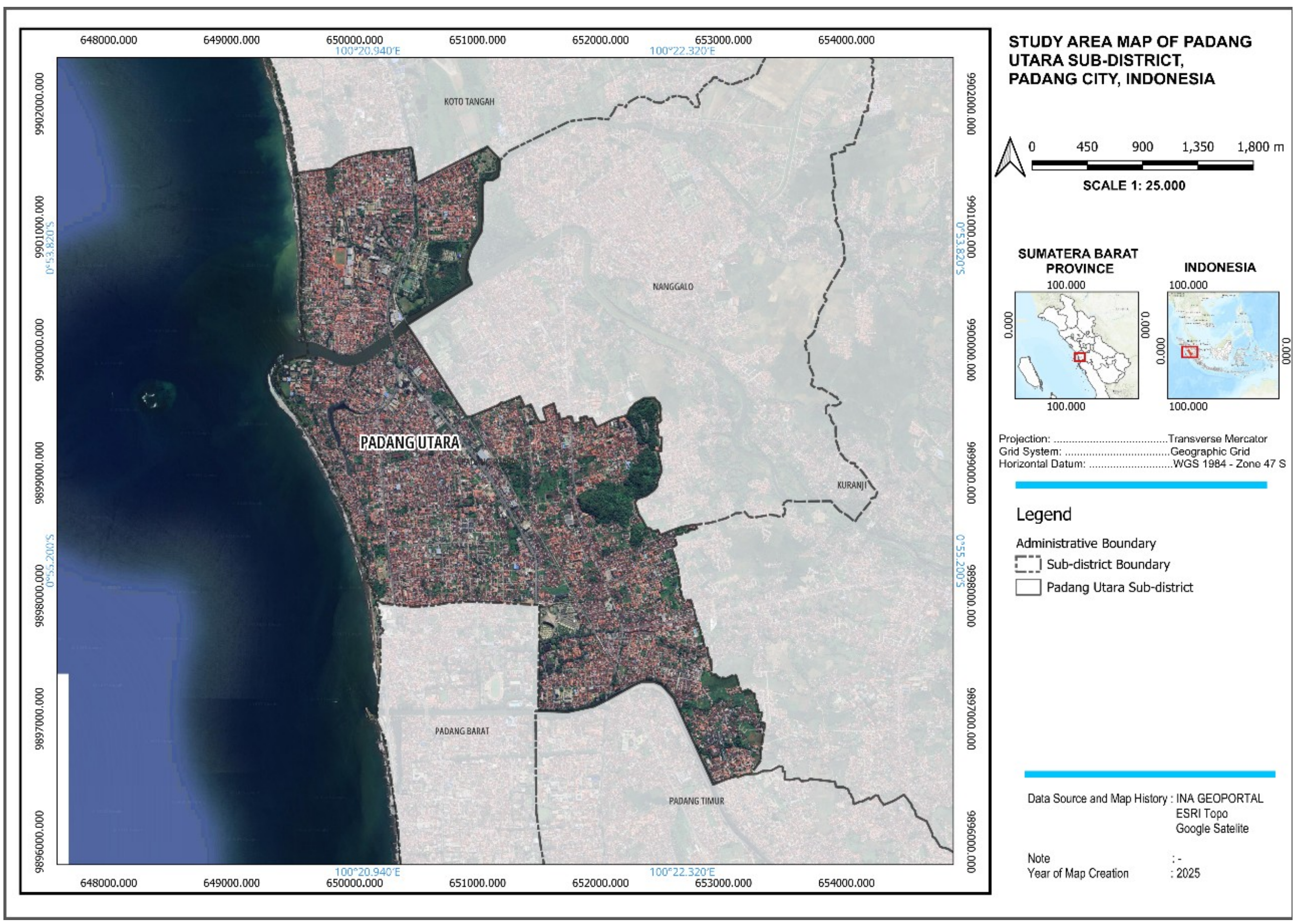

Figure 1. Study Area of Padang utara Subdistrict, Padang City

consists of seven subdistricts. This subdistrict is bordered by Kuranji Subdistrict to the east and the Indian Ocean to the west, Koto Tangah and Naggalo Subdistricts to the north, and Barat and Timur Padang Subdistricts to the south [19]. This subdistrict is home to many government offices, commercial centers, and educational institutions, making it one of the most densely populated subdistricts in Padang City (Fultriasantri & Fajrin, 2023; Peraturan Wali Kota Padang Nomor 5 Tahun 2023 Tentang Rencana Detail Tata Ruang Kota Padang Tahun 2023 - 2043, 2023). The location can be seen in more detail in **Fig.** (1).

2.2 Tools and Materials

a) Tools

Data processing and analysis in this study were conducted using three main platforms. Google Earth Engine (GEE) was used to process DSM data using the multi-temporal hillshadow function to obtain dynamic shadow analysis. The QGIS application (v. 3.34.12) served as the main tool for spatial data analysis and visualization, including meteorological data interpolation (IDW), data aggregation using zonal statistics, and final calculation of correction factors through field calculators. Third, the Python programming language on the Google Collab platform was used to perform statistical analysis and data visualization of the processing results [22][23].

b) Materials

This study utilizes monthly shortwave radiation (SWR) data from JAXA's Himawari-8 satellite as input for calculating solar radiation in 2024 [24]. Building height data was obtained from Google Open Building 2.5 D open source data with a resolution of 1 m [16]. This data was then combined with canopy height data from Meta and WRI [17], as well as Fabdem from Copernicus to obtain Digital Surface Model (DSM) data for the Padang Utara subdistrict. Building footprint data was obtained from OpenStreetMap (OSM) open source data, monthly air temperature data for 2024 sourced from the Meteorology, Climatology, and Geophysics Agency (BMKG), and wind speed data from NASA Power, which was then analyzed using Inverse Distance Weighting (IDW) to obtain the distribution of monthly air temperature and wind speed in the Padang Utara subdistrict for 2024 [25], [26], [27].

2.3 Data Processing

a) Meteorological Correction Factor

To obtain effective solar PV output, meteorological factors are important parameters that must be considered [28]. Therefore, meteorological correction factor analysis is essential to obtain rooftop solar PV potential that is more in line with field conditions. This study uses the Japanese Industrial Standards (JIS) approach as a reference framework with several modifications based on contemporary studies by [13]. Previous studies have shown that an increase in module temperature (cell temperature) can significantly reduce the power output of solar PV [29]. Therefore, the first step in this study was to model the impact of meteorological factors (in this case, temperature and wind) on the potential reduction in rooftop solar PV capacity. The data used was solar radiation or short wave radiation (SWR) data from the Himawari-8 satellite, combined with air temperature and wind speed data that had undergone inverse distance weighting (IDW) analysis.

The analysis of meteorological factors begins with the calculation of wind effects. Wind can increase efficiency by cooling the modules and blowing away dust that accumulates on the solar PV [12], [30]. To calculate the effect of wind speed on solar panels, the following **Eq. (1)**. can be used:

$$Wind\ effect = \frac{9.5}{5.7+3.8V} \tag{1}$$

Where V is wind speed in (m/s).
In the next step, the module temperature (Tc) is calculated using the following **Eq. (2).**

$$T_c = T_a + \frac{I_{tot}}{I_{NOCT}}(T_{NOCT} - T_{aNOCT}) \times windeffect \tag{2}$$

Where Tc is the cell temperature and Ta is the air temperature in Celsius (C). Itot is the total irradiation data reaching the earth's surface (W/m^2), I_{NOCT} is the irradiation at the Nominal Operating Cell Temperature in this study set at 800 Watts, T_{NOCT} is the temperature at the Nominal Operating Cell Temperature in this study valued at (45 °C) [29], [31], and T_{aNOCT} is the air temperature under NOCT conditions in this study, used as the value of (20 °C) [29].

After obtaining the cell temperature analysis, the calculation of the decrease in solar cell performance caused by temperature (TempLoss) or meteorological correction factors is continued using the **Eq. (3).**

$$Temp_{Loss} = 1 + \beta_{ref}(T_c - T_s) \tag{3}$$

Where T_c is the cell temperature and T_s is the temperature under standard test conditions (25°C) and β_{ref} is the efficiency correction coefficient for temperature (/C), which in this study is set at −0.0045/C [31].

b) *Urban Geometric Correction Factor*

The shadow factor from buildings and vegetation is also an important consideration for the effectiveness of rooftop solar PV output in urban areas. The presence of taller trees and buildings casts shadows on smaller buildings, reducing the amount of direct sunlight they receive [32]. Two parameters are used to assess this impact: shaded area and sky view factor.

To determine the dynamically shaded area, this study uses the ee.Terrain.hillshadow function on the Google Earth Engine (GEE) cloud computing platform. This platform was chosen because it can perform large-scale spatial data processing in parallel and is well suited for intensive multi-temporal analysis. Unlike conventional hillshade, which only produces static visualizations, hillshadow can generate shadowed areas based on the sun's position at a specific time, represented in binary form where 0 denotes shadowed areas and 1 denotes illuminated areas [33].

The position of the sun (azimuth and zenith angles) in this study was extracted using the pvlib.location.Location Python function from the pvlib library on the Google Collab platform [34]. This analysis was conducted at seven representative times throughout the day (7:00 a.m., 9:00 a.m., 11:00 a.m., 12:00 p.m., 2:00 p.m., 3:00 p.m., and 5:00 p.m.) on the 15th of each month [34], [35]. This data is then aggregated by summing it up and dividing it by the total observation time, so that the values on the map become continuous data ranging from 0 (always shaded) to 1 (always sunny). This data illustrates the duration of time a location is exposed to direct sunlight or shade. This calculation applies the formula used in the study [36].

In addition to the shading factor, another important parameter in urban climate analysis is the Sky View Factor (SVF). The Sky View Factor can be defined as an index that describes the proportion of open sky visible from a particular position, which directly affects longwave radiation. This value is represented on a scale of 0 to 1, where 0 indicates a completely covered sky and 1 indicates a completely open sky. In this study, the SVF was obtained using the Sky View Factor tool in the QGIS application, with a Digital Surface Model (DSM) as the input data [37].

These two parameters are then integrated to obtain the urban geometric correction factor (UGCF), which considers the availability of direct radiation represented by the Shading Factor (SF) and the availability of diffuse radiation represented by the SVF. In this study, an equation was formulated that combines these two parameters, supported by research [38], [39]. This study reveals the importance of shadow analysis and SVF in determining the potential of rooftop solar PV with the following **Eq. (4).**

$$UGCF = (\alpha \times SF) + \big((1-\alpha) \times SVF\big) \tag{4}$$

Where UGCF is the Urban Geometric Correction Factor and α is the weighting coefficient in this study, which is 0.5 based on research [40] that assesses the proportion of direct and diffuse radiation in tropical regions. Furthermore, SF is the Shading Factor (value 0-1) describing the contribution of direct radiation. SVF is the Sky View Factor (value 0-1), representing the fraction of unobstructed sky for diffuse radiation reception.

c) *Optimal Location of Solar PV Potential*

The third stage of this study is to determine the optimal location for rooftop solar PV by combining existing parameters using zonal statistics tools on building footprints, which are then calculated using the previous equations through a field calculator.

To determine the optimal location for rooftop solar PV, an equation was used that refers to the Japanese Industrial Standards (JIS) approach, which was then modified based on several previous studies [13], [38], [39] with the following **Eq. (5).**

$$PV_{Optimal} = I_{tot} \times Temp_{Loss} \times UGCF \times PCS_{Loss} \times System_{Loss} \times Capacity \tag{5}$$

Where I_{tot} is the total radiation reaching the earth's surface, $Temp_{Loss}$ is the decrease in solar cell performance due to temperature, UGCF is the effect of decreased solar cell performance due to urban geometry. Then PCS_{Loss} is the reduction caused by the power conditioning system, which in this study will be determined to be 0.95. $System_{Loss}$ is the reduction due to the PV system, which in this study will be set at 0.95 [41], [42]. The capacity of the solar cell in this study is set at 1 (Kwp).

The results of the analysis were then classified into five classes using natural breaks (Jenks), which grouped the data based on its natural distribution into the following classes: very less optimal, less optimal, moderately optimal, optimal, and very optimal [43].

The complete analysis process can be seen in **Fig.** (2).

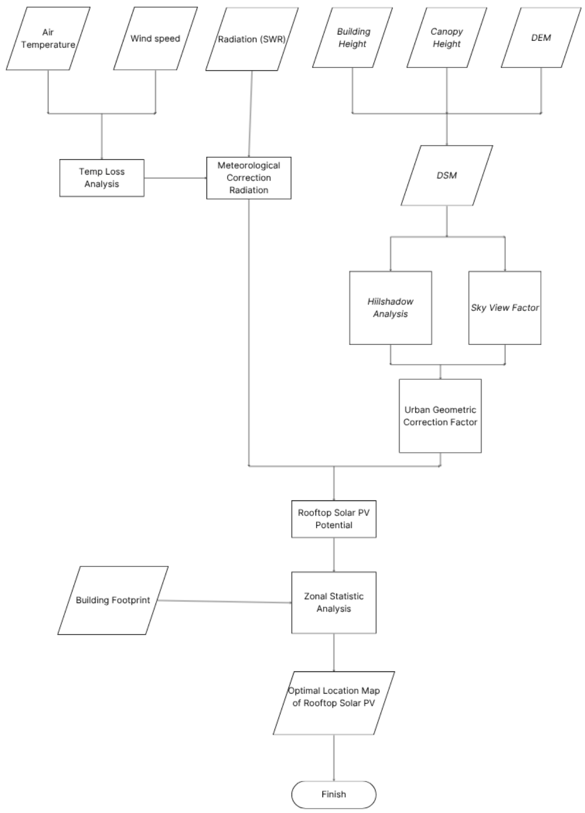

Figure 2. Research Flow Chart

III. RESULT AND DISCUSSION

3.1 Meteorological Correction Factor Analysis

Accurate analysis of rooftop solar PV potential requires correction for meteorological factors that affect solar panel performance in the field. The main factor modeled in this study is performance loss due to temperature (Temperature Loss), which depends on the operating temperature of the solar cell (Tc).

From this data, a clear seasonal pattern can be observed, influenced by local climatic conditions. The cell operating temperature (Tc) shows the highest average values during the period from February to April, peaking in February (average 33.78 °C). This period coincides with the annual apparent motion of the sun, which is located in the southern hemisphere and close to the city of Padang, which generally has high solar radiation and warm air temperatures. Conversely, the lowest cell temperature was recorded in December (average 30.7 °C), which aligns with the peak of the rainy season.

These temperature variations directly impact the energy conversion efficiency of PV panels. The performance loss factor (TempLoss) is calculated based on these conditions, where a value of 1.0 represents 100% efficiency and lower values indicate losses. The analysis results show that the most significant performance loss occurs in February, where the average panel efficiency drops to 96.05% from its standard efficiency. Conversely, the panel's optimal performance is recorded in December, where its efficiency reaches 97.42% with an average annual efficiency decline of 3.64%.

The low Tc and TempLoss variations in Padang are directly related to the relatively small air temperature variation pattern. This condition is supported by research conducted by [44] which states that the temperature increase was only around 0.01°C per year during 2010–2019.

Although monthly TempLoss variations appear small (ranging between 1-2%), their impact is cumulative and significant in calculating annual energy potential. Ignoring this factor will result in an overestimation of the potential that can be generated. Therefore, integrating this meteorological correction factor is a basic step to ensure a more realistic and accountable estimate of rooftop solar PV potential. **Tab. (1).** presents a summary of monthly statistics for these two parameters across the study area.

3.2 Urban Geometric Correction Factor Analysis

In addition to meteorological factors, the main limiting factor for the potential of rooftop solar PV in urban environments is the geometry of the built environment itself. To calculate the combined impact of direct shading and sky view factor, an Urban

Geometric Correction Factor (UGCF) is calculated for each building. The monthly distribution of UGCF across the study area is presented in a box plot in **Fig. (3).**

This visualization reveals two contrasting key findings. First, the majority of roofs in Padang Utara Subdistrict show excellent geometric quality. This is evident from the median position (center line of the box) which consistently remains above 0.88 for all months. Furthermore, 75% of the total roofs (first quartile and above) have a UGCF value above 0.82. This indicates that most roofs in the study area are relatively open and not overly affected by shadows from surrounding buildings, demonstrating strong basic potential for rooftop solar PV development.

Second, on the other hand, this graph also clearly identifies the existence of a significant subpopulation of roofs with poor geometric quality. This is represented by the numerous outliers scattered below each box plot, with some roofs even having UGCF values below 0.5. These roofs are the locations most affected by shadow effects, likely due to being in narrow alleys, near taller buildings or vegetation, or experiencing significant self-shading due to complex architecture. Lower UGCF values are more commonly found around campus areas, office buildings, commercial centers, and a small portion of areas adjacent to green open spaces.

TABLE 1 DESCRIPTIVE STATISTICS FOR CELL TEMPERATURE AND TEMP LOSS IN PADANG UTARA SUBDISTRICT

	Cell Temperature (Tc)				TempLoss			
Month	Min	Max	Mean	Std	Min	Max	Mean	Std
January	32.529	33.350	33.03317	0.252314	0.962	0.966	0.963818	0.001177
February	33.466	34.049	33.77566	0.150494	0.959	0.962	0.960484	0.000735
March	32.528	33.491	33.04214	0.248975	0.962	0.966	0.963711	0.001238
April	33.146	34.164	33.63548	0.255950	0.959	0.963	0.961121	0.001256
May	32.348	33.325	32.82825	0.246711	0.963	0.967	0.964821	0.001211
June	32.338	33.226	32.79089	0.224220	0.963	0.967	0.964890	0.001187
July	32.934	33.726	33.36396	0.205975	0.961	0.964	0.962356	0.000986
August	31.163	32.325	31.77143	0.297818	0.967	0.972	0.969640	0.001260
September	31.823	32.539	32.20018	0.183121	0.966	0.969	0.967550	0.000946
October	32.690	33.315	33.06587	0.171833	0.963	0.965	0.963650	0.000835
November	32.082	32.777	32.44928	0.179383	0.965	0.968	0.966374	0.000980
December	30.408	30.973	30.69442	0.143516	0.973	0.976	0.974179	0.000722

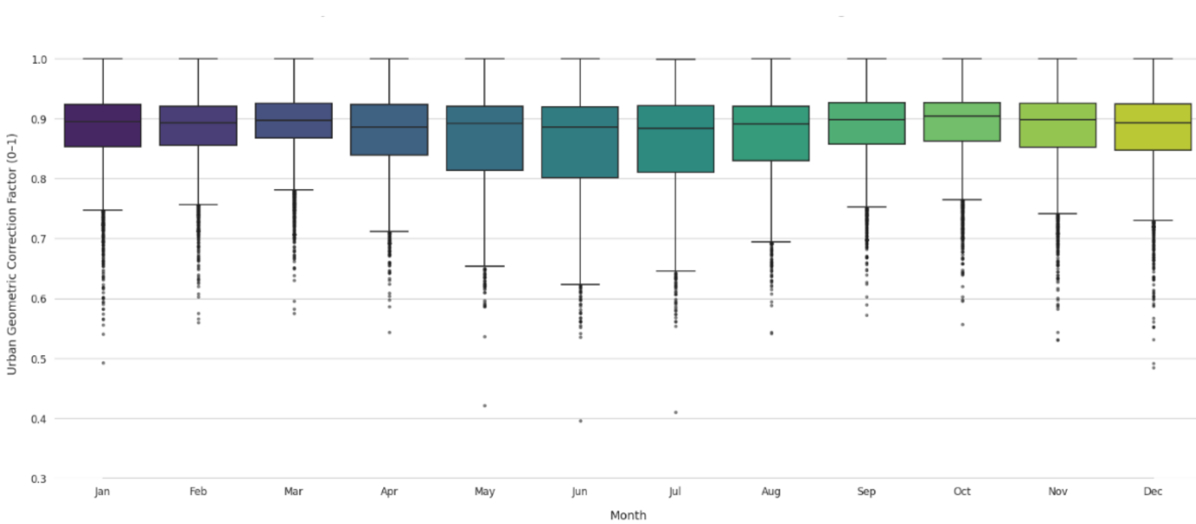

Figure 3. Box Plot Monthly Urban geometric Corection Factor at Padang Utara Subdistrict, Padang City

This condition is in line with research [45] stating that shadow correction factors around commercial areas can have a correction factor of 0.6. The average annual percentage loss in output was 11.77%. This is much lower than the average decline in Kingston, Canada, which was 27% [14]. For further details, refer to the monthly aggregated shading factor map in **Fig. (4).**

This finding emphasizes the importance of conducting detailed analysis to identify suboptimal locations in the planning process.

Finally, subtle seasonal variations were observed in the distribution of UGCF. A slight decrease in the median value and interquartile range was detected during the June-August and December-January periods. This phenomenon is related to annual changes in the position of the sun. When the sun is lower in the sky during the northern and southern solstices, shadows tend to be longer because the sun's position tends to move away from the city of Padang, thereby reducing the average radiation quality across all districts compared to the equinox periods (March-April and September-October) [9], [46].

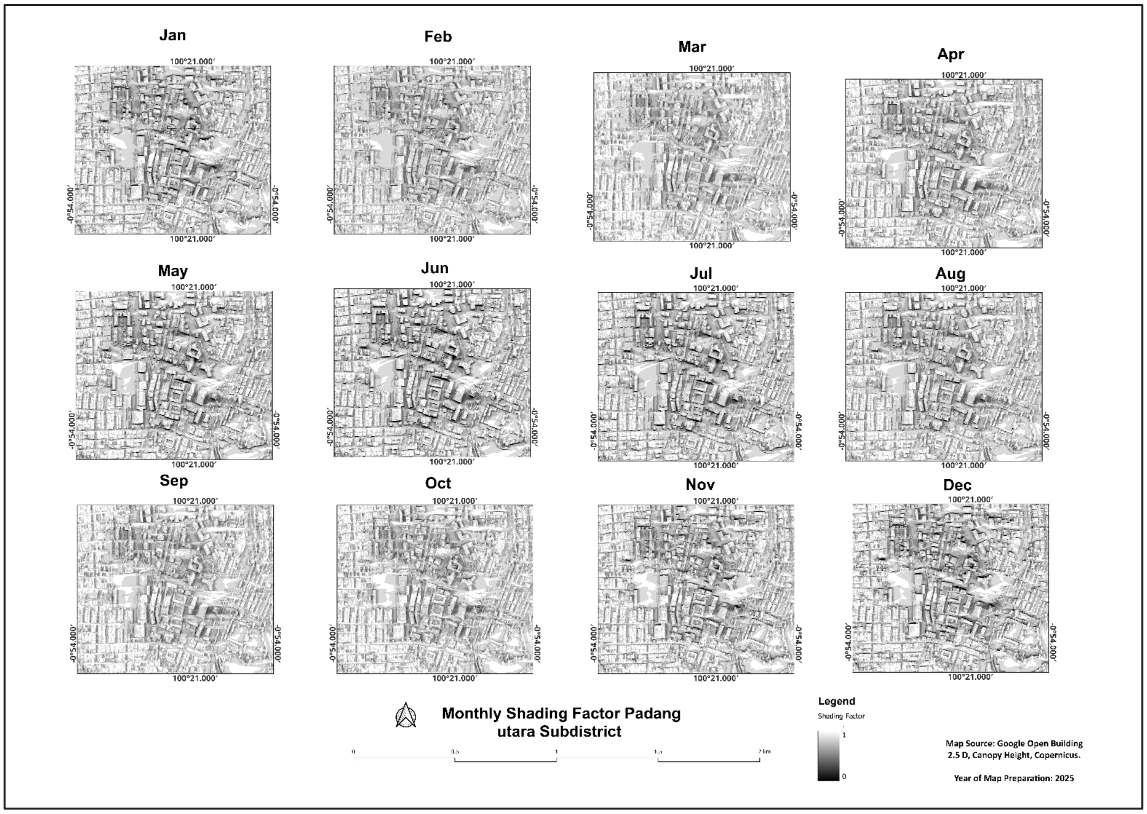

Figure.4 Monthly Shading Factor Aggregat at Padang Utara Subdistrict, Padang City

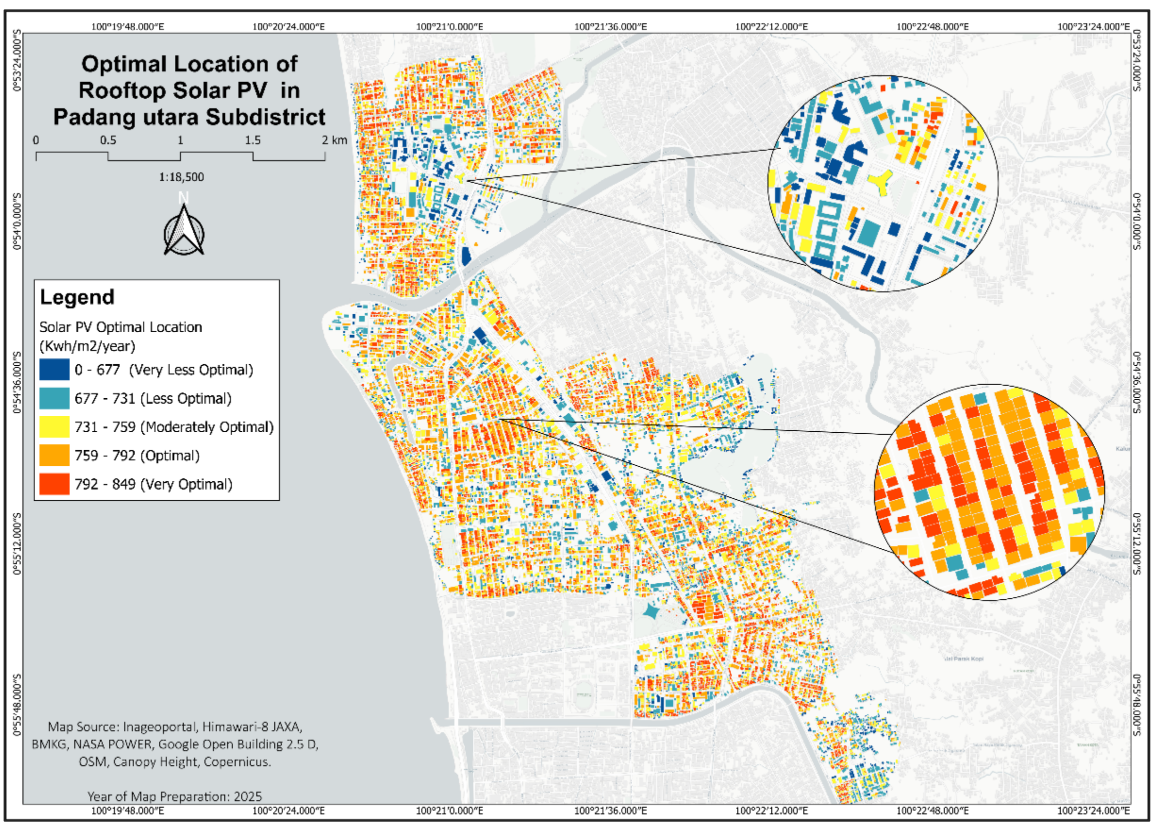

Figure.5 Optimal Location of Rooftop Solar PV at Padang Utara Subdistrict, Padang City

3.3 Spatial Distribution of Optimal Rooftop Solar PV Potential

The culmination of this research is the integration of all meteorological and geometric correction factors to produce the final Optimal Location Map of Rooftop Solar PV for the Padang Utara Subdistrict, as presented in **Fig. (5).** This map spatially visualizes the annual solar energy potential (kWh/m²/year) classified into five levels of optimality using the Natural Breaks (Jenks) method. The summary of this classification is provided in **Tab. (2)**. The analysis reveals that a significant portion of the rooftops in the study area are highly suitable for solar PV installation. A combined 47.17% of all viable buildings fall into the 'Optimal' (35.91%) with the range of radiation is (758.8 – 792.03 Kwh/m^2/year) and 'Very Optimal' (11.26%) or (792.03 – 848.63 Kwh/m^2/year) categories. These approximately 47,803 rooftops represent the primary locations with the highest potential energy yield, making them priority areas for future solar energy development programs and incentives.

The spatial patterns revealed in the map are strongly correlated with the urban morphology discussed previously. As highlighted in the lower inset of **Fig. (5)** the highest potential rooftops (colored orange and red) are predominantly concentrated in residential areas characterized by simpler, lower-profile building structures. These areas benefit from minimal self-shading and less obstruction from neighboring buildings.

Conversely, areas with lower potential (colored blue and cyan), such as the university campus area shown in the upper inset, are characterized by larger, architecturally complex buildings. Despite their height, these buildings exhibit lower potential per square meter due to significant self-shading, where taller parts of the structure cast shadows onto lower sections of the same roof. This finding underscores a critical insight: building height alone is not an indicator of high solar potential; rather, architectural simplicity and minimal shading are the dominant factors [47]. Office and commercial areas show the same pattern. In addition to being influenced by the surrounding high-rise buildings, self-shading is also a factor that deserves attention.

To see the optimal monthly radiation pattern, refer to **Fig. (6).**

TABLE 2 CLASSIFICATION OPTIMAL LOCATION OF ROOFTOP SOLAR PV PADANG UTARA SUBDISTRICT

Class Range (Kwh/m^2/year)	Number of Buildings	Percentage (%)
Very Less Optimal (487.07 – 677.08)	9113	8.99
Less Optimal (677.08 – 730.3)	23014	22.71
Moderately Optimal (730.3 – 758.8)	21409	21.13
Optimal (758.8 – 792.03)	36393	35.91
Very Optimal (792.03 – 848.63)	11410	11.26

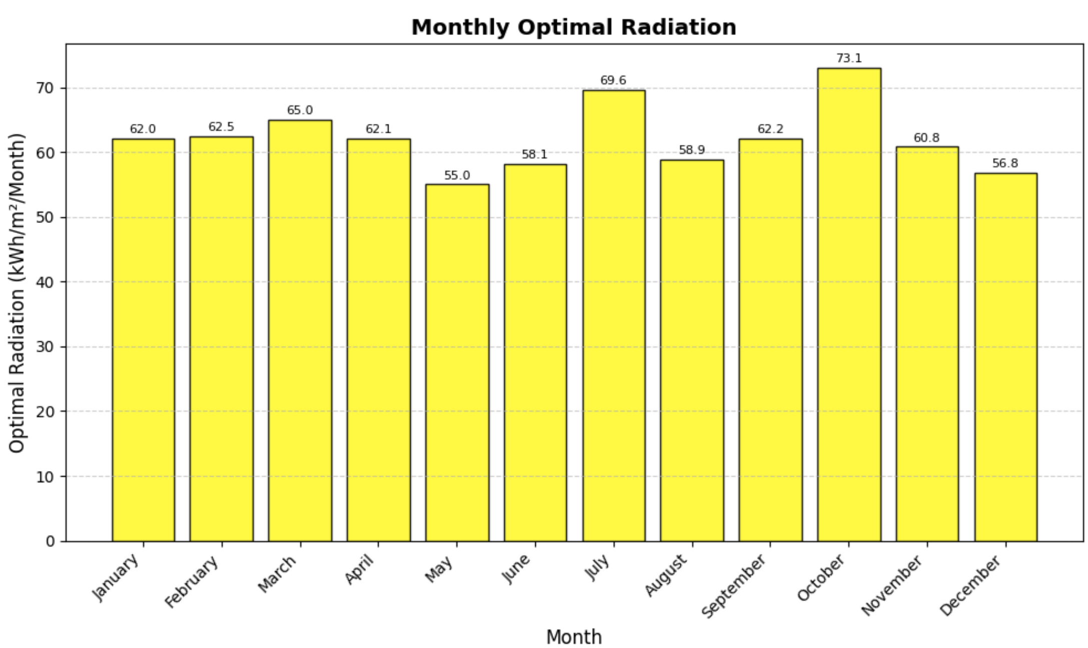

Figure.6 Monthly Optimal Radiation at Padang utara Subdistrict, Padang City

Furthermore, the monthly variability of solar potential was analyzed. The total available optimal radiation across the subdistrict shows a distinct seasonal pattern, with the highest solar resource availability in October (73.08 kWh/m²) and the lowest in May (55.02 kWh/m²). This temporal variation is a crucial consideration for energy grid planning, indicating periods of peak and reduced solar generation throughout the year.

Although this study has generally been able to determine the optimal location for rooftop solar power plants, it still has some limitations in terms of the detail of the data used to capture the geometry of the roof, and it has not taken into account the area of the roof that is suitable based on the existing slope. This could be a suggestion for further research.

IV. CONCLUSION

This study has developed and applied high-resolution spatial analysis to map the optimal potential of rooftop solar PV in dense tropical urban environments, using fully open-source data and cloud computing based. By integrating detailed meteorological correction factors and urban geometric factors, this model provides more realistic estimates than conventional macro-scale approaches.

The main findings indicate that Padang Utara subdistrict has enormous potential for decentralized solar energy development. Quantitatively, it was found that 47.17% of the total technically feasible roofs fall into the ‘Optimal’ and ‘Very Optimal’ categories with radiation (758.8–792. 03 kWh/m²/year) and (792.03–848.63 kWh/m²/year), indicating priority locations for development. The analysis also revealed that while meteorological factors such as temperature cause an annual performance reduction of approximately 3.64%, the most significant limiting factor is urban geometry 11.77%.

The most important scientific contribution of this study is the identification of the phenomenon of internal roof shading (self-shading) as a dominant factor that reduces the potential of large buildings with complex architecture. Contrary to the common assumption that taller buildings have the best potential, this study proves that roofs on lower buildings with simpler structures, such as those in residential areas, often offer higher energy efficiency.

However, this study also acknowledges its limitations, namely that open source data cannot fully capture the variations in building roofs, so that analysis of roof slopes and roof geometry, which tend to be complex, has not been included in the analysis.

ACKNOWLEDGEMENT

The author sincerely thanks all my colleagues, open source geospatial data providers: JAXA, Google, Meta, WRI, Copernicus, OSM, BMKG, and NASA for providing open source data, as well as the Google Earth Engine team for the powerful cloud computing platform that made this research possible.

REFERENCES

[1] W. F. Lamb *et al.*, “A review of trends and drivers of greenhouse gas emissions by sector from 1990 to 2018,” Jul. 01, 2021, *IOP Publishing Ltd*. doi: 10.1088/1748-9326/abee4e.

[2] E. Papadis and G. Tsatsaronis, “Challenges in the decarbonization of the energy sector,” Aug. 15, 2020, *Elsevier Ltd*. doi: 10.1016/j.energy.2020.118025.

[3] S. Rauner, F. Piontek, B. Soergel, and G. Luderer, “The impact of energy sector pollution on human development and inequality amidst climate change,” *Environmental Research Letters*, vol. 19, no. 9, Sep. 2024, doi: 10.1088/1748-9326/ad6b39.

[4] K. Obaideen *et al.*, “Solar Energy: Applications, Trends Analysis, Bibliometric Analysis and Research Contribution to Sustainable Development Goals (SDGs),” Jan. 01, 2023, *Multidisciplinary Digital Publishing Institute (MDPI)*. doi: 10.3390/su15021418.

[5] T. M. Kibtiah, G. D. P. Dewi, A. Bainus, M. F. Abdurrahman, D. Rhasan, and K. M. Suitela, “Solar Energy in Indonesia: The Implementation of Sustainable Development Goals for Net Zero Emissions,” in *IOP Conference Series: Earth and Environmental Science*, Institute of Physics, 2024. doi: 10.1088/1755-1315/1324/1/012093.

[6] D. Bernasconi and G. Guariso, “Rooftop PV: Potential and Impacts in a Complex Territory,” *Complex Territory. Energies*, p. 14, 2021, doi: 10.3390/en.

[7] Z. Zhang *et al.*, “Carbon mitigation potential afforded by rooftop photovoltaic in China,” *Nat Commun*, vol. 14, no. 1, Dec. 2023, doi: 10.1038/s41467-023-38079-3.

[8] D. Pan, Y. Bai, M. Chang, X. Wang, and W. Wang, “The technical and economic potential of urban rooftop photovoltaic systems for power generation in Guangzhou, China,” *Energy Build*, vol. 277, Dec. 2022, doi: 10.1016/j.enbuild.2022.112591.

[9] D. Triana, I. Garniwa, A. H. Y. Rosadi, and D. N. Martono, “Performance Analysis Simulation of Urban Rooftop Photovoltaic Potential in Jakarta City, Indonesia,” *Environmental Research, Engineering and Management*, vol. 80, no. 4, pp. 21–38, 2024, doi: 10.5755/j01.erem.80.4.34200.

[10] D. F. Silalahi, A. Blakers, M. Stocks, B. Lu, C. Cheng, and L. Hayes, “Indonesia’s vast solar energy potential,” *Energies (Basel)*, vol. 14, no. 17, Sep. 2021, doi: 10.3390/en14175424.

[11] X. Huang, K. Hayashi, T. Matsumoto, L. Tao, Y. Huang, and Y. Tomino, “Estimation of Rooftop Solar Power Potential by Comparing Solar Radiation Data and Remote Sensing Data—A Case Study in Aichi, Japan,” *Remote Sens (Basel)*, vol. 14, no. 7, Apr. 2022, doi: 10.3390/rs14071742.

[12] O. Bamisile, C. Acen, D. Cai, Q. Huang, and I. Staffell, “The environmental factors affecting

solar photovoltaic output," Feb. 01, 2025, *Elsevier Ltd*. doi: 10.1016/j.rser.2024.115073.

[13] K. T. N. Ihsan, A. D. Sakti, A. Higuchi, H. Takenaka, and K. Wikantika, "City-Level Solar Photovoltaic Potential Using Integrated Surface Models and Himawari Satellite in Jakarta and Bandung Indonesia," *Energy Build*, vol. 319, Sep. 2024, doi: 10.1016/j.enbuild.2024.114552.

[14] H. T. Nguyen and J. M. Pearce, "Incorporating shading losses in solar photovoltaic potential assessment at the municipal scale," *Solar Energy*, vol. 86, no. 5, pp. 1245–1260, May 2012, doi: 10.1016/j.solener.2012.01.017.

[15] L. Sander, D. Schindler, and C. Jung, "Application of Satellite Data for Estimating Rooftop Solar Photovoltaic Potential," *Remote Sens (Basel)*, vol. 16, no. 12, Jun. 2024, doi: 10.3390/rs16122205.

[16] W. Sirko *et al.*, "High-Resolution Building and Road Detection from Sentinel-2," Sep. 2024, [Online]. Available: http://arxiv.org/abs/2310.11622

[17] J. Tolan *et al.*, "Very high resolution canopy height maps from RGB imagery using self-supervised vision transformer and convolutional decoder trained on aerial lidar," *Remote Sens Environ*, vol. 300, Jan. 2024, doi: 10.1016/j.rse.2023.113888.

[18] M. Amani *et al.*, "Google Earth Engine Cloud Computing Platform for Remote Sensing Big Data Applications: A Comprehensive Review," *IEEE J Sel Top Appl Earth Obs Remote Sens*, vol. 13, pp. 5326–5350, 2020, doi: 10.1109/JSTARS.2020.3021052.

[19] Badan Pusat Statistik Kota Padang, "Kecamatan Padang Utara Dalam Angka 2024," 2024.

[20] I. Fultriasantri and Fajrin, "INTERPRETASI HIBRID CITRA SENTINEL-2A DI KOTA PADANG," Apr. 2023. doi: https://doi.org/10.35580/jes.v5i2.43339.

[21] WALI KOTA PADANG PROVINSI SUMATERA BARAT, *Peraturan Wali Kota Padang Nomor 5 Tahun 2023 Tentang Rencana Detail Tata Ruang Kota Padang Tahun 2023 - 2043*. Indonesia, 2023.

[22] QGIS Development Team, "QGIS Geographic Information System," 2023, *QGIS Association*: 3.34.12.

[23] Google, "Google Colaboratory," 2025, *Google*.

[24] Japan Aerospace Exploration Agency, "Himawari-8/9 L3 Monthly Shortwave Radiation (SWR)," JAXA. Accessed: May 17, 2025. [Online]. Available: https://www.eorc.jaxa.jp/ptree/index.html

[25] BMKG, "Data Suhu Udara Online," BMKG. Accessed: Aug. 02, 2025. [Online]. Available: https://dataonline.bmkg.go.id/dataonline-home

[26] NASA Prediction of Worldwide Energy Resources (POWER) Project, "Monthly Wind Speed at 10 m," NASA. Accessed: Jun. 13, 2025. [Online]. Available: https://power.larc.nasa.gov/data-access-viewer/

[27] OpenStreetMap contributors, "OpenStreetMap." Accessed: May 10, 2025. [Online]. Available: https://www.openstreetmap.org/#map=5/-2.55/118.02

[28] K. Hasan, S. B. Yousuf, M. S. H. K. Tushar, B. K. Das, P. Das, and M. S. Islam, "Effects of different environmental and operational factors on the PV performance: A comprehensive review," Feb. 01, 2022, *John Wiley and Sons Ltd*. doi: 10.1002/ese3.1043.

[29] E. Skoplaki, A. G. Boudouvis, and J. A. Palyvos, "A simple correlation for the operating temperature of photovoltaic modules of arbitrary mounting," *Solar Energy Materials and Solar Cells*, vol. 92, no. 11, pp. 1393–1402, Nov. 2008, doi: 10.1016/j.solmat.2008.05.016.

[30] Z. R. Tahir *et al.*, "Effect of Temperature and Wind Speed on Efficiency of Five Photovoltaic Module Technologies for Different Climatic Zones," *Sustainability (Switzerland)*, vol. 14, no. 23, Dec. 2022, doi: 10.3390/su142315810.

[31] J. Adeeb, A. Farhan, and A. Al-Salaymeh, "Temperature effect on performance of different solar cell technologies," *Journal of Ecological Engineering*, vol. 20, no. 5, pp. 249–254, 2019, doi: 10.12911/22998993/105543.

[32] H. Waqas, Y. Jiang, J. Shang, I. Munir, and F. U. Khan, "An Integrated Approach for 3D Solar Potential Assessment at the City Scale," *Remote Sens (Basel)*, vol. 15, no. 23, Dec. 2023, doi: 10.3390/rs15235616.

[33] N. Gorelick, M. Hancher, M. Dixon, S. Ilyushchenko, D. Thau, and R. Moore, "Google Earth Engine: Planetary-scale geospatial analysis for everyone," *Remote Sens Environ*, vol. 202, pp. 18–27, Dec. 2017, doi: 10.1016/j.rse.2017.06.031.

[34] R. W. Andrews, J. S. Stein, C. Hansen, and D. Riley, "Introduction to the open source PV LIB for python Photovoltaic system modelling package," in *2014 IEEE 40th Photovoltaic Specialist Conference, PVSC 2014*, Institute of Electrical and Electronics Engineers Inc., Oct. 2014, pp. 170–174. doi: 10.1109/PVSC.2014.6925501.

[35] T. Hong, M. Lee, C. Koo, K. Jeong, and J. Kim, "Development of a method for estimating the rooftop solar photovoltaic (PV) potential by analyzing the available rooftop area using Hillshade analysis," *Appl Energy*, vol. 194, pp. 320–332, May 2017, doi: 10.1016/j.apenergy.2016.07.001.

[36] A. D. Sakti *et al.*, "Multi-Criteria Assessment for City-Wide Rooftop Solar PV Deployment: A Case Study of Bandung, Indonesia," *Remote*

Sens (Basel), vol. 14, no. 12, Jun. 2022, doi: 10.3390/rs14122796.

[37] J. Bernard, E. Bocher, G. Petit, and S. Palominos, "Sky view factor calculation in urban context: Computational performance and accuracy analysis of two open and free GIS Tools," *Climate*, vol. 6, no. 3, Sep. 2018, doi: 10.3390/cli6030060.

[38] X. Lu, G. Li, L. Zhou, L. Hao, G. Lv, and B. Lin, "Photovoltaic potential estimation for various surface components of urban residential buildings based on Industry Foundation Classes data," *Energy Sci Eng*, vol. 10, no. 10, pp. 3741–3765, Oct. 2022, doi: 10.1002/ese3.1253.

[39] G. Desthieux *et al.*, "Solar energy potential assessment on rooftops and facades in large built environments based on lidar data, image processing, and cloud computing. Methodological background, application, and validation in geneva (solar cadaster)," *Front Built Environ*, vol. 4, Mar. 2018, doi: 10.3389/fbuil.2018.00014.

[40] O. S. Ojo, "Effect of Climate Change on Solar Radiation over a Tropical Region," in *2021 International Conference on Decision Aid Sciences and Application, DASA 2021*, Institute of Electrical and Electronics Engineers Inc., 2021, pp. 332–337. doi: 10.1109/DASA53625.2021.9682407.

[41] H. Ohtake, F. Uno, T. Oozeki, Y. Yamada, H. Takenaka, and T. Y. Nakajima, "Estimation of satellite-derived regional photovoltaic power generation using a satellite-estimated solar radiation data," *Energy Sci Eng*, vol. 6, no. 5, pp. 570–583, Oct. 2018, doi: 10.1002/ese3.233.

[42] K. Kawajiri, T. Oozeki, and Y. Genchi, "Effect of temperature on PV potential in the world," *Environ Sci Technol*, vol. 45, no. 20, pp. 9030–9035, Oct. 2011, doi: 10.1021/es200635x.

[43] S. Li and J. Shan, "Adaptive Geometric Interval Classifier," *ISPRS Int J Geoinf*, vol. 11, no. 8, Aug. 2022, doi: 10.3390/ijgi11080430.

[44] E. G. Ekaputra, E. Stiyanto, and N. A. I. Hasanah, "Surface temperature across land-use change phenomena in Padang, Indonesia," in *IOP Conference Series: Earth and Environmental Science*, IOP Publishing Ltd, May 2021. doi: 10.1088/1755-1315/757/1/012037.

[45] J. Byrne, J. Taminiau, L. Kurdgelashvili, and K. N. Kim, "A review of the solar city concept and methods to assess rooftop solar electric potential, with an illustrative application to the city of Seoul," 2015, *Elsevier Ltd*. doi: 10.1016/j.rser.2014.08.023.

[46] J. Wang, "Solar Shadow Positioning Based on Quadratic Function Fitting," 2017.

[47] A. Aronescu and J. Appelbaum, "Shading on photovoltaic collectors on rooftops," *Applied Sciences (Switzerland)*, vol. 10, no. 8, Apr. 2020, doi: 10.3390/APP10082977.